RESEARCH PAPER

Gadoterate meglumine - anionic linear globular dendrimer second generation: A novel nano sized theranostic contrast agent

Noorin Yousefiyeh [1], Abolfazl Arab [1], Elnaz Salehian [1], Radin Alikhani [2], Shabnam Samimi [1], Artin Assadi [1], Mehdi Shafiee Ardestani [1]*

[1]Department of Radiopharmacy, Faculty of Pharmacy, Tehran University of Medical Sciences, Tehran, Iran
[2]Department of Medicinal Chemistry, School of Pharmacy, Ardabil University of Medical Sciences, Ardabil, Iran

ABSTRACT

Objective(s): Cancer is known as one of the most life-threatening diseases in the world. Early diagnosis of cancer may significantly increase the chance of effective treatment. In the recent years, the importance of medical imaging usage has been increased to identify cancer's nature and pattern of growth in order to provide the most advantageous treatment approaches for cancer tumors. Magnetic resonance imaging is an efficient non-invasive tool for early diagnosis of cancer which provides clear scans of various tissues without radiation. Contrast Agents such as Gadoterate Meglumine enhance contrast MR imaging and provide imaging from inside the cells without entering them.
Materials and Methods: In this study, Gadoterate Meglumine nano-sized anionic linear globular dendrimer second generation was first synthesized and then qualitative and quantitative methods were carried out to ensure the proper synthesis and to assess the toxicity of the compound. Once the non-toxicity of the chemical was ensured, *in vivo* MR imaging studies was performed to test the impact of the synthesized compound on the resolution of image.
Results: The result obtained from this study demonstrated that the attachment of Gadolinium (III) to a nano dendrimer reduces its cytotoxicity and also improved resolution of image. In this research, Gadoterate Meglumine nano-sized anionic linear globular dendrimer second generation was effectively able to enter the cells while showing low cytotoxicity in the normal cells and moderate cytotoxicity on cancer cells.
Conclusion: Therefore, $ALGDG_2$-GM could be introduced as a novel, safe, effective and promising nano-sized theranostic contrast agent candidate.

Keywords: Cancer, Diagnostic; MRI, Nanoparticle, Therapeutic

INTRODUCTION

Cancer is known as the second cause of death and is predicted to become the leading cause of death in the next few years and surpassing heart disease [1,2]. Imaging techniques are the most significant tools for early diagnosis of many cancers [3,4]. Nowadays, molecular imaging is playing an important role in the diagnosis and monitoring efficacy of therapy in some diseases like cancer (A). The most common techniques used for imaging modalities are positron emission tomography (PET), single photon emission computed tomography (SPECT), computed tomography, ultrasound imaging, and MRI [5]. These techniques are used to provide either functional/molecular information or anatomical information from the target tissue. Owing to the high contrast resolution of MR imaging technique, this method has been widely used as a non-invasive diagnostic imaging tool for internal tissue imaging [6,7].

MRI contrast agents (CA) are a group of chemical compounds that enhance the clarity of MR contrast imaging. Gadoterate meglumine (Dotarem®) is a gadolinium-based contrast agent (GBCA) used for MR imaging [8]. GBCAs differ in a number of properties, such as chemical structure

(linear versus macrocyclic), thermodynamic stability, kinetic stability (i.e., time course of dissociation of gadolinium), ionicity, concentration, osmolality, viscosity, pharmacokinetics, and relaxivity (a measure of their ability to enhance tissue during MRI exams) these characteristics have implications for diagnostic performance safety [9]. As gadolinium-based contrast agents have low relaxivity and a high dose of agents is required, they may cause severe side effects such as nephrogenic systemic fibrosis (NSF) [10]. Therefore, there is an increasing demand for contrast agents with relatively high relaxivity, low dose of administration and mild side effects in clinic.

Another fundamental limitation of conventional contrast agents is reported to be their poor sensitivity. Therefore, there is a need for a highly sensitive contrast agent for more accurate imaging [11]. Recently, using nanocarriers in clinical therapeutics and diagnostic applications has gained so much attractions. To date, nanoparticles have been widely used in researches as a suitable tool to overcome the traditional obstacles like rapid clearance, poor half-life, non-targeted distribution and poor contrast and resolution with reporting breakthrough results in molecular imaging, especially when it comes to non-invasive methods for cancer cell therapy and imaging [12-16]. High surface area-to-volume ratio, target-specific delivery of drugs, decreasing drug toxicity and increasing drug solubility are attributed to nanocarriers making them an effective drug delivery system with an outstanding performance [15].

Among nanocarriers, dendrimers have been paid a particular attention for the molecular imaging of target tissues. Being a class of highly branched and symmetrical supramolecular scaffolds, dendrimers consist of repeating dendrons extending outward from a central core [17]. Dendrimers are polymers synthesized reproducibly with low polydispersity, a highly desirable feature in drug delivery vehicles, and in a controlled manner, yielding products with predictable sizes termed as "generation". In order to carry out desired *in vivo* pharmacokinetic requirements for intended biomedical applications, different generations of dendrimers can be designed and exploited [18]. As previously mentioned, dendrimers are advantageous for drug delivery purposes. Owing to the exponential increase in the number of peripheral groups while dendrimer's core branches out in the synthesis of each generation, the resulting shielded interior can be used as a capsule to load drugs for delivery. Inevitably, the amine or carboxylate peripheral functional groups can be used in conjugation with functional molecules in a multivalent format to amplify the imaging signal and enhance the therapeutic efficacy [19]. Undoubtedly, dendrimers can be used as nano scaffolds for bioactive agents to develop theranostic agents for oncologic applications owing to their unique structural features. Consequently, branched structure and dense surface functional groups make dendrimers suitable for efficient drug delivery.

Dendrimer-based contrast agents used for MRI have the potential to improve the resolution of MR images and the pharmacokinetic profile of contrast agents as a result of being able to carry high CA payload which means CA dose minimization for high quality imaging [20,21]. Anionic linear globular dendrimer contains some advantages in drug delivery application over other polymeric dendrimers such as PAMAM, chitosan and PLGA, such as biodegradability, biocompatibility and substantial water solubility [22,23].

The term *theranostic* refers to a mixture of diagnostic and therapeutic function as a single entity for a single nanoparticle [24]. Recently, using dendrimers as a cancer theranostic nanocarrier in MRI has been investigated [25]. In this study, our group would like to introduce $ALGDG_2$-GM as a novel nano-sized theranostic contrast agent to target both diagnosis and treatment approaches in cancer. The chemical structure of ALGD was confirmed by proton nuclear magnetic resonance (HNMR), Fourier transform infrared spectroscopy (FT-IR) and liquid chromatography–mass spectrometry (LC/MS). GM-$ALGDG_2$ synthesis was confirmed by size distribution and zeta potential evaluation with DLS (dynamic light scattering). The cellular toxicity of $ALGDG_2$-GM was evaluated by XTT (2,3-bis-(2-methoxy-4-nitro-5-sulfophenyl)-2H-tetrazolium-5-carboxanilide) assay on both normal and cancerous cell lines. Furthermore, cellular drug uptake by the cancerous cell lines was evaluated by inductively coupled plasma-atomic emission spectroscopy (ICP-AES). To assess the enhancement of imaging, both *in vitro* and *in vivo* MRI assays were done.

MATERIALS AND METHODS
Synthesis of GM-ALGDG₂

$ALGDG_2$ was synthesized according to our

Nanomed. J. 8(4): 298-306, Autumn 2021

299

previous report [26]. After confirming ALGDG$_2$ synthesis with FT-IR (NEXUS 870; Thermo Fisher Scientific, Waltham, MA, USA), HNMR (Bruker Corporation, Billerica, MA, USA) and LC/MS (Agilent 6410 Triple Quadrupole LC/MS) analyses, two concentrations of ALGDG$_2$ (X=7.26 ml and 2X=14.5 ml) were prepared to observe whether toxicity is dependent to dendrimer concentration.

In order to load GM on ALGDG$_2$, 2 mmole of GM, purchased from Bayer HealthCare Pharmaceuticals (Inc, Montville, NJ, USA), was mixed with X and 2X concentrations of ALGDG$_2$ to make two different dilutions named X ALGDG$_2$-GM and 2X ALGDG$_2$-GM, respectively. The mixture was allowed to stir at pH=7-7.5 for at least 2 hr. Both dilutions were sonicated for 15 min with a sonicator (Bandelin/ Sonorex RK100 model). Afterwards, to remove excess free Gd3+ ions, the reaction pH was increased to 9 and free Gd3+ ion was precipitated and filtered. To increase the purity the reaction mixture was dialyzed. To confirm the synthesis of ALGDG$_2$-GM, zeta potential and size distribution of ALGDG$_2$ before and after GM loading for both X ALGDG$_2$ and 2X ALGDG$_2$ were calculated by DLS (Nano ZS, Malvern).

In vitro cytotoxicity analysis

Human Embryonic Kidney (HEK-293) cell line and Human Glioblastoma Cell Culture (HGCC) were purchased from national Cell Bank of Iran (Pasteur Institute, Tehran, Iran). Both cell lines were cultured at 37 °C in 5% carbon dioxide (CO$_2$) humidified incubator while each of them was cultured in RPMI 1640 medium supplementing with 10% fetal bovine serum and 1% Penicillin/ Streptomycin. To evaluate cell viability, XTT assay was performed according to proliferation kit II (XTT) (Roche Applied Science, Germany) instruction. Cell viability/toxicity of ALGDG$_2$, X ALGDG$_2$-GM, 2X ALGDG$_2$-GM and free GM at the same concentration (150 μg/ml) was calculated on each cell line after 72 hr using an automated microplate reader (BioTek Instruments, USA) at 570 nm.

In vitro cellular uptake measurement

HGCC cell line was cultured until the concentration reaches 2×10^5 cells per well. Afterwards, cells were replaced and incubated with ALGDG$_2$, X ALGDG$_2$-GM, 2X ALGDG$_2$-GM and free GM at the same concentration (150 μg/ml) at 37 °C and 5% CO$_2$ for 24 hr in three wells. After

incubation, cells were washed 3 times with 500 μL of PBS, centrifuged at 1500 rpm for 15 min and reestablished in 2 mL of cell culture media. At the end, cellular uptake of each sample solution was measured quantitatively by ICP-AES.

Analysis of MRI

A 1.5 Tesla General Electric (US) piece of device (from Rajaei Cardiac Center Hospital, Tehran, Iran) was used in the case of measurements on MRI. Different concentrations of X ALGDG$_2$-GM including 0.125, 0.625, 0.031, 0.0156 and 0.0078 mg/ml alongside with distilled water (as a blank) and equal doses of magnetization - as the standard sample - were provided. T1-weighted MRI at 1.5 T intensity was determined by the means of multipoint method and analysis of the exponential curve for signal intensity against Repetition Time (TR) according to the protocol (Standard spin echo: number of echoes=32, TE=13/26/39/52/66/79/92/105/118/145/158/171/184/198/211/237/250/264/277/290/303/330/343/356/369/382/396/422ms, TR=20/50/100/200/400/2000/3000ms, Matrix=256*256, Slice Thickness=1/5mm, FOV=18*18cm, NEX=Non). The relaxation time of T1 was computed with MATLAB (1.0.0.1 version) and Microsoft Excel 2007 software.

In vivo MRI imaging

An 8-week-old Syrian mouse with breast cancer was used for *in vivo* MR imaging. The mouse was received a 0.1 ml of ketamine and xylazine mixtures to be anesthetized. After anesthesia, it was fixed with a tape on an imaging film. After fixation, whole-body MR imaging was taken using 1.5 T MRI device. Then, a 0.2 mL/kg of X ALGDG$_2$-GM was injected intravenously to the mouse and whole-body MR imaging was repeated to compare the contrast and the resolution of the images before and after injection. The signals of MR imaging were visualized by DICOM (Digital Imaging and Communication in Medicine) software version 1.3.5 (Digital Imaging and Communications in Medicine, Rosslyn, VA, USA).

Statistical analysis

Statistical data analysis was performed using Prism 5 and Microsoft Excel 2013 software. For the quantitative data analysis, One-way ANOVA was applied for cluster comparison. $P<0.05$ was considered statistically significant.

300

Nanomed. J. 8(4): 298-306, Autumn 2021

RESULTS

Confirmation of GM-ALGDG*$_2$ *synthesis by spectroscopy studies

FT-IR, HNMR and LC/MS confirmed successful synthesis of ALGDG$_2$. For more clarification, readers are referred to the spectrums demonstrated in Fig. 1-3.

Result of mass spectrometry (LC-MS) for the ALGDG$_2$ has been shown in Fig 1. According to the spectrum and our knowledge about the model of mass cleavages in PEG-containing structures to produce repetitive PEG-containing units, the resulting peaks can successfully interpret the formation of ALGDG$_2$.

Result of FT-IR spectrometry for the ALGDG$_2$ is observed in Fig 2. FT-IR spectroscopy is useful for several types of analysis as there are no two unique molecular structures producing the same FT-IR spectrum. According to Fig 1. The peaks between 3200 and 3600 cm^{-1} are related to NH and OH groups. The peak 1590–1760 cm^{-1} wavelength explicit carbonyl groups of the compound, aliphatic carbon-hydrogen peaks at 2600–3000 cm^{-1}, and 1726.27 cm^{-1} peak that exclusively depicts the dendrimer.

Result of Proton-NMR spectroscopy (H NMR) of ALGDG$_2$ is depicted in Fig 3. All hydrogen can be easily observed and calculated from the peaks' The
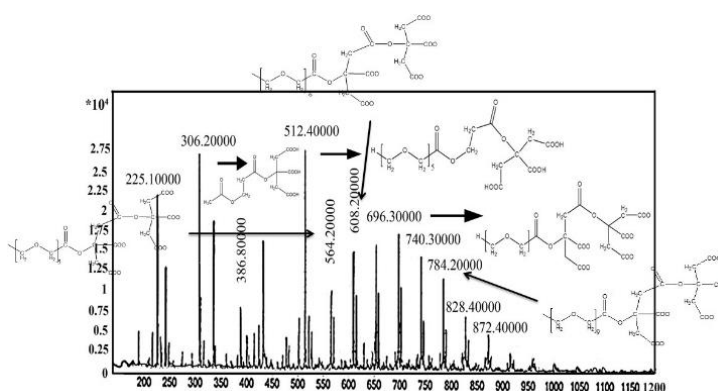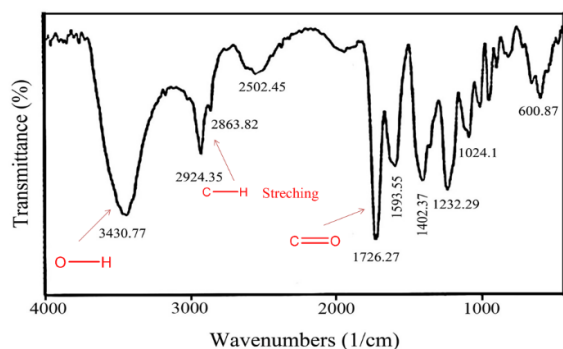

Fig 1. LC/MS spectrum of ALGDG2

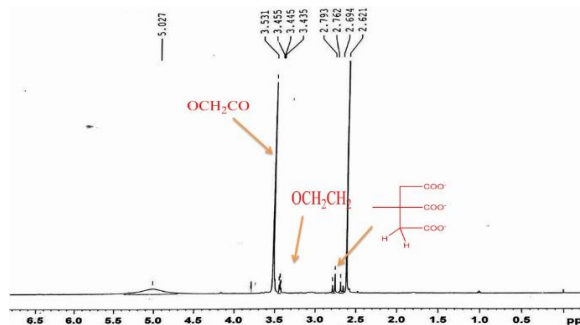Figure 2. FT-IR spectrum of ALGDG2

Fig 3. H NMR spectrum of ALGDG2

integrals. The chemical shifts δ 2.5 and 3.5 δ are related to the citric acid and polyethylene glycol moieties in the dendrimer structure, respectively. These chemical shifts verify the synthesis of ALGDG2 molecule.

Comparative results exhibited that ALGDG2 size was increased after GM loading both in X ALGDG2-GM and 2X ALGDG2-GM. However, the increase in

size for 2X ALGDG2-GM was more significant than X ALGDG2-GM (Fig 4). After GM loading, ALGDG2 was negatively charged both in X ALGDG2-GM and 2X ALGDG2-GM. However, 2X ALGDG2-GM was more negatively charged than X ALGDG2-GM (Fig 5). The observed variation in size distribution and zeta potential successfully confirmed the synthesis of both X ALGDG2-GM and 2X ALGDG2-GM. The
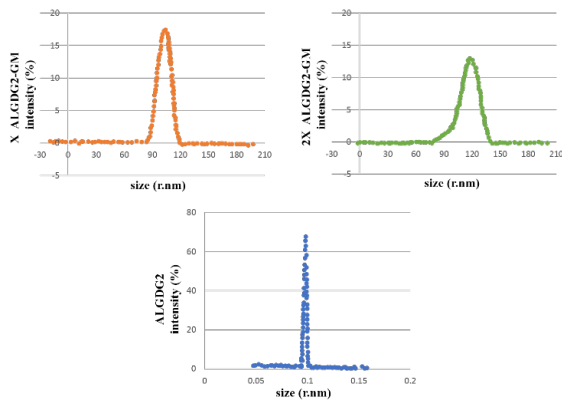
Nanomed. J. 8(4): 298-306, Autumn 2021

301

Fig 4. Dispersion curve for size distribution as a function of intensity (%) orange: X ALGDG2-GM, green: 2X ALGDG2-GM, blue: ALGDG2

schematic $ALGDG_2$-GM loading can be illustrated in Fig 6.

In vitro cytotoxicity and cellular uptake evaluation

Results of XTT assay on both HEK-293 and HGCC cell lines could be observed in Figure 7. It was eminently obvious that while both concentrations
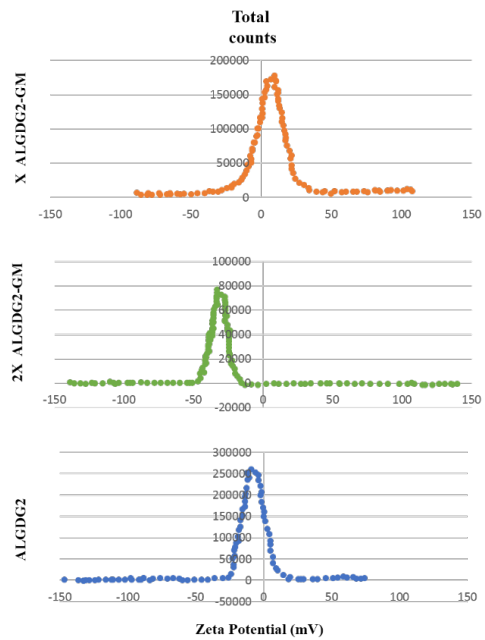

Fig 5. Dispersion curve for zeta potential with regard to total counts
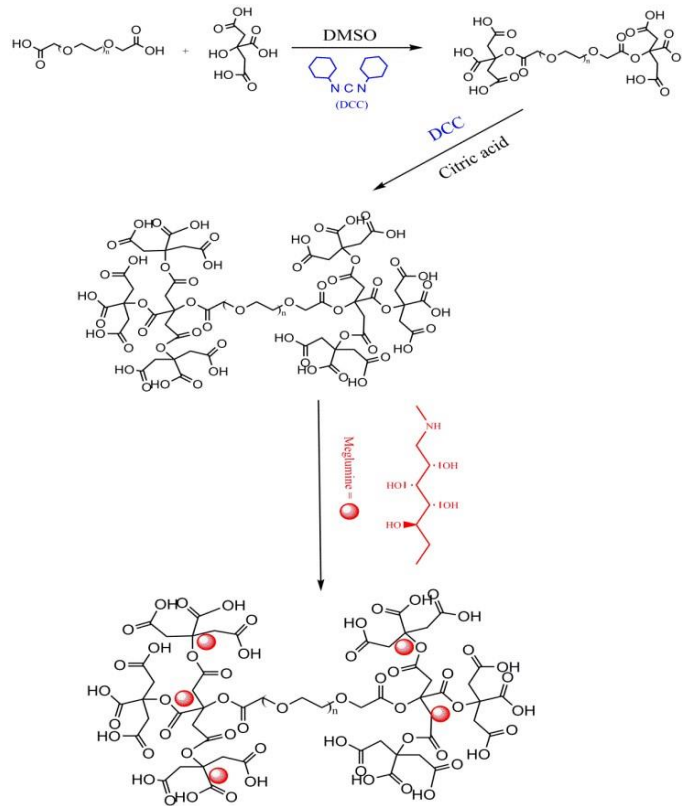orange: X ALGDG2-GM, green: 2X ALGDG2-GM, blue: ALGDG2

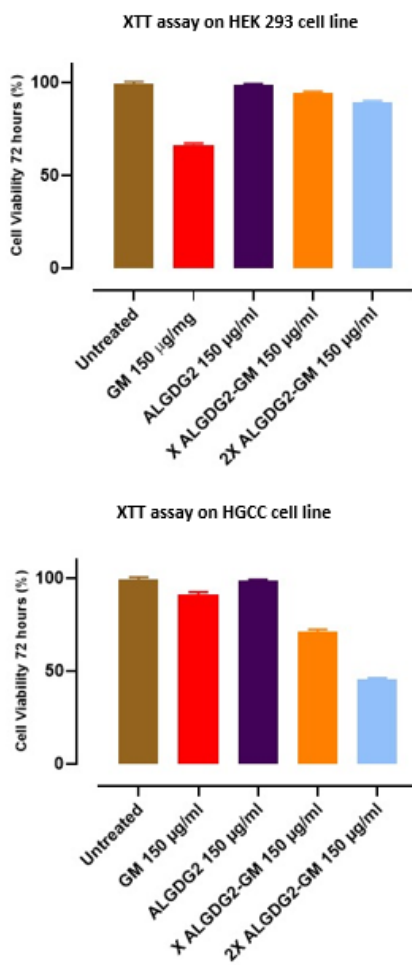Fig 6. schematic illustration of ALGDG2-GM loading

XTT assay on HEK 293 cell line

XTT assay on HGCC cell line

Fig 7. XTT assay. HGCC cells line was exposed to the samples for 72 hr

HGCC Cellular uptake%

Fig 8. HGCC cells line cellular uptake

of ALGDG$_2$-GM were non-toxic on HEK-293, GM exhibited an approximate toxicity on the similar cell line. Surprisingly, in the case of HGCC, whereas GM created a little toxicity, both concentrations of -GM were notably toxic and 2X ALGDG$_2$-GM was far more poisonous than X ALGDG$_2$-GM. ALGDG$_2$ was non-toxic on both cell lines. Furthermore, HGCC cellular uptake result illustrated that the poor ability of GM to enter the cells was dramatically enhanced after ALGDG$_2$ loading, particularly in 2X ALGDG$_2$-GM rather than X ALGDG$_2$-GM (Fig 8).

DISCUSSION

The current study revealed a successful strategy in generating a powerful nano-biomolecular probe by using the biocompatibility and appropriate Gd (III) loading capability for both *in vitro* and *in vivo* MR imaging.

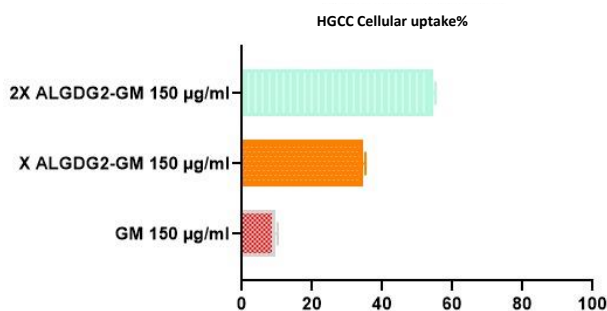It is estimated that GBCA is eliminated in blood after 90 min. However, recent reports have shown that it still remains in some tissues causing a potential health risk subjected to the free Gadolinium toxicity. The *in vitro* cytotoxicity analysis of this study confirmed moderate toxicity of GM as a GBCA on the normal cell lines. The toxicity was dramatically decreased when it was loaded on ALGDG$_2$. Surprisingly, GM displayed low inhibition on HEK-293 and HGCC cancer cell lines. However, this inhibition was increased notably after GM was loaded on ALGDG$_2$. Two concentrations were also used to evaluate the intracellular uptake and potential use for *in vitro* and *in vivo* molecular imaging in cancer cells. The data showed that the cancer inhibitory profile of ALGDG$_2$-GM is concentration-dependent in which the toxicity of 2X ALGDG$_2$-GM far outweighs X ALGDG$_2$-GM. The major hurdles of using GBCA for imaging might be its poor specificity and cellular uptake. The novel nanosized ALGDG$_2$-GM was proved to tackle this barrier according to our elucidated data. The low cellular uptake of GM was dramatically increased after it was loaded on ALGDG$_2$. The confirming data showed that the increased uptake of 2X ALGDG$_2$-GM by the cancerous cells, compared to X ALGDG$_2$-GM, heralds the dose-dependent effect of tumor inhabitation. This is supported by comparing the variation between size and zeta potential of X ALGDG$_2$-GM and 2X ALGDG$_2$-GM. According to the collected data, the zeta potential was approximately -17.7 mV for X ALGDG$_2$-GM and -24.3 mV for 2X ALGDG$_2$-GM, respectively. In addition, the size distribution for X ALGDG$_2$-GM was 104.9 nm and for 2X ALGDG$_2$-GM was 117.9 nm.

Results show that there is a concentration range in which the zeta-potential is affected by nanoparticle concentration. 2X ALGDG$_2$-GM was more negatively charged than X ALGDG$_2$-GM. This is accompanied by the onset of aggregation of
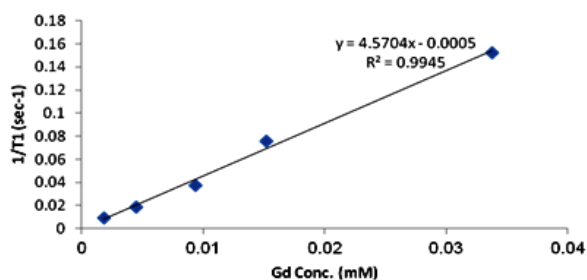
Nanomed. J. 8(4): 298-306, Autumn 2021

303

Fig 9. The r1 relaxivity curve of X ALGDG2-GM

Fig 10. MR images (A) pre-injection and (B) 60-min post-injection

the nanoparticles, made evident by an increase in the mean particle size measured. The increase in particle size that accompanied the observed shift in values of zeta potential may be explained by the nature of the PCS (photon correlation spectroscopy) optics, rather than the occurrence of particle aggregation. In most PCS instruments, including the Malvern Zeta sizer, the optics operates in a homodyne mode. This usually implies that there is no external reference light received by the photodetector. However, when scattering from the nanoparticles themselves is very weak (in this case due to the decrease in nanoparticle concentration), then other sources of scattered light will become a significant part of the detected light. These other sources include not only the scattering from water molecules but more importantly, any stray light from the cell wall at the spot where incident and scattering light enter or exit. The signal will thus be composed of a homodyne term and a heterodyne term, which will ultimately be interpreted by the software as larger particle size.

It had been previously proved that Gd (III) complexes can conjugate to dendrimer's peripheral functional groups to result a significant enhancement in relaxivity [19]. By considering the aforementioned fact and MRI studies in this project, T1-weighted MRI for X ALGDG$_2$-GM demonstrated a large longitudinal (r1) (Fig 9). It revealed an increase in T1 that confirmed the contrast image enhancement. Accordingly, X ALGDG$_2$-GM has shortened T1 relaxation time to maximize its T1 contrast effect that results in a brightening of the MR image. Pre-injection and 60 min post-injection MR images can be found in Fig 10. Clearly, there seems to be a significant enhancement in the contrast and resolution, markedly in the cancerous area.

One of the advantages of the ALGDG$_2$ is its PEG core which makes it mostly attractive to cancerous cells as well as anticancer effects. The presence of citric acid shell in ALGDG$_2$ is another advantage as it gives an interesting capability to ALGDG$_2$ to raise potent Gd (III) complex formation as well as Gd (III) loading. In addition, nanoprobe is protected from any toxic surface-surface interactions between the normal cell body and the conjugate by the negative charge of dendrimer G2 [27].

One of the main criteria of biomolecular conjugation is to not producing any biological activity disturbances. These disturbances usually occur when one or both active sites (covering kinetic or dynamic) of biomolecules suffer from an inactivation. Based on the obtained *in vitro* observations here, GM serves its activity after dendrimer conjugation and this fact leads to next nano-conjugate *in vivo* success, Thus, gadolinium loaded nanoconjugate (ALGDG$_2$-GM) was founded quite successful in all the biological experiments performed [28].

CONCLUSION

In this study, therapeutic and imaging characteristics of novel nano theranostic CA, ALGDG$_2$-GM, were presented for the first time. Results confirmed that ALGDG$_2$-GM would be considered as a promising nano-sized CA for both therapy and imaging purposes with regard to its biocompatibility, inexpensive synthesis, high degree of cellular uptake, enhanced MR imaging, non-toxic effect on normal cells and tumor inhibitory effect in comparison with GM. The results of MRI studies showed an enhancement in contrast and resolution of imaging when ALGDG$_2$-GM was applicated.

Although chemotherapy has long been

304

performed to treat various types of cancer, combination of MR contrast agent and drug is predicted to overcome many limitations of conventional chemotherapy such as low targeting efficacy and side effects [29,30]. To date, many chemotherapy drugs have been seen in the construction of dendrimer-based drug delivery vehicles, which include Curcumin, Genistein, Cisplatin, PTX, Resveratrol, DOX, Camptothecin (CPT), MTX, Indomethacin, and Paclitaxel [19]. In this regard, various magnetic nanoparticles (MNP) have been developed to enhance the diagnosis via compensating the low contrast effect and low specific treatment efficacy caused in chemotherapy. MNPs like dendrimers can be used as a suitable MR contrast agent due to their super-paramagnetic property. MNPs seem to be very competent for drug delivery and diagnostic purposes. In order to carry various molecules and to release in a specific environment, they can be derivated from particles of various sizes and properties.

Recently, magnetic nanoparticles have been taken into account to overcome the drawbacks of CA usage including rapid clearance, poor half-life, non-targeted distribution and poor contrast and resolution, particularly in non-invasive methods for chemotherapy and imaging. Among nanoparticles, dendrimers could be considered as a great fit in practice as a nanoparticle-based CA due to their special physiochemical characteristics such as highly branched structure, water solubility, low toxicity, biocompatibility, polydispersity and biodegradability [31-33]. Since GM-ALGDG$_2$ was introduced as a safe, effective and promising nanoparticle-based contrast agent to target cancer cells for both clinical imaging and therapeutic purposes, we hope the results of this study would be useful for further studies in design and synthesis of novel nano dendrimer-based theranostic contrast agents (e.g. Gd (III)-dendrimer complex derivatives) to be used in different imaging applications.

STATEMENT OF ETHICS

This study was approved by the ethical committee of Tehran University of the Medical Science Council.

ACKNOWLEDGMENTS

CONFLICT OF INTEREST

All authors declare that the study has not any conflict of interest.

REFERENCES

1. Stewart BW, Bray F, Forman D, Ohgaki H, Straif K, Ullrich A, Wild CP. Cancer prevention as part of precision medicine: 'plenty to be done'. Carcinogenesis. 2016;37(1):2-9.
2. Siegel RL, Miller KD, Jemal A. Cancer Statistics. CA Cancer J Clin. 2017;67(1):7-30.
3. Anand P, Kunnumakkara AB, Sundaram C, Harikumar KB, Tharakan ST, Lai OS, Sung B, Aggarwal BB. Cancer is a preventable disease that requires major lifestyle changes. Pharm Res. 2008; 25(9):2097-2116.
4. Cibiel A, Pestourie C, Ducongé F. *In vivo* uses of aptamers selected against cell surface biomarkers for therapy and molecular imaging. Biochimie. 2012;94(7):1595-1606.
5. Anderson CJ, Lewis JS. Current status and future challenges for molecular imaging. Philos Trans A Math Phys Eng Sci. 2017;375(2107):20170023.
6. Wu M, Shu J. Multimodal Molecular Imaging: Current Status and Future Directions. Contrast Media Mol Imaging. 2018; 2018:1382183.
7. Hermann P, Kotek J, Kubícek V, Lukes I. Gadolinium(III) complexes as MRI contrast agents: ligand design and properties of the complexes. Dalton Trans. 2008; (23): 3027-47.
8. Rogosnitzky M, Branch S. Gadolinium-based contrast agent toxicity: a review of known and proposed mechanisms. Biometals. 2016;29(3):365-376.
9. Zhou Z, Lu ZR. Gadolinium-based contrast agents for magnetic resonance cancer imaging. Wiley Interdiscip Rev Nanomed Nanobiotechnol. 2013;5(1):1-18.
10. Perazella MA. Current status of gadolinium toxicity in patients with kidney disease. Clin J Am Soc Nephrol. 2009; 4(2):461-469.
11. Kim J, Lee N, Hyeon T. Recent development of nanoparticles for molecular imaging. Philos Trans A Math Phys Eng Sci. 2017;375(2107):20170022.
12. Mohammadi E, Amanlou M, Ebrahimi SES, Hamedani MP, Mahrooz A, Mehravi B, Emami BA, Aghasadeghi MR, Bitarafan AR, Pouraliakbar HR, Ardestani MS. Cellular uptake, imaging and pathotoxicological studies of a novel Gd [III]–DO3A-butrol nano-formulation. Rsc Advances. 2014; 4(86): 45984-45994.
13. Naseri N, Ajorlou E, Asghari F, Pilehvar-Soltanahmadi Y. An update on nanoparticle-based contrast agents in medical imaging. Artif Cells Nanomed Biotechnol. 2018;46(6): 1111-1121.
14. Patra JK, Das G, Fraceto LF, Campos EVR, Rodriguez-Torres MDP, Acosta-Torres LS, Diaz-Torres LA, Grillo R, Swamy MK, Sharma S, Habtemariam S, Shin HS. Nano based drug delivery systems: recent developments and future prospects. J Nanobiotechnology. 2018;16(1):71.
15. Din FU, Aman W, Ullah I, Qureshi OS, Mustapha O, Shafique S, Zeb A. Effective use of nanocarriers as drug delivery systems for the treatment of selected tumors. Int J Nanomedicine. 2017;12:7291-7309.

Nanomed. J. 8(4): 298-306, Autumn 2021

305

16. Ding L, Lyu Z, Dhumal D, Kao CL, Bernard M, Peng L. Dendrimer-based magnetic resonance imaging agents for brain cancer. Sci China Mater. 2018;61(11):1420-1443.

17. Svenson S, Tomalia DA. Dendrimers in biomedical applications--reflections on the field. Adv Drug Deliv Rev. 2005;57(15):2106-2129.

18. Gillies ER, Fréchet JM. Dendrimers and dendritic polymers in drug delivery. Drug Discov Today. 2005;10(1):35-43.

19. Lo ST, Kumar A, Hsieh JT, Sun X. Dendrimer nanoscaffolds for potential theranostics of prostate cancer with a focus on radiochemistry. Mol Pharm. 2013;10(3):793-812.

20. Zhu Y, Liu C, Pang Z. Dendrimer-Based Drug Delivery Systems for Brain Targeting. Biomolecules. 2019;9(12): 790.

21. Singh AP, Biswas A, Shukla A, Maiti P. Targeted therapy in chronic diseases using nanomaterial-based drug delivery vehicles. Signal Transduct Target Ther. 2019;4:33.

22. Sandoval-Yañez C, Castro Rodriguez C. Dendrimers: Amazing Platforms for Bioactive Molecule Delivery Systems. Materials (Basel). 2020;13(3):570.

23. Fana M, Gallien J, Srinageshwar B, Dunbar GL, Rossignol J. PAMAM Dendrimer Nanomolecules Utilized as Drug Delivery Systems for Potential Treatment of Glioblastoma: A Systematic Review. Int J Nanomedicine. 2020;15:2789-2808.

24. Dong Q, Yang H, Wan C, Zheng D, Zhou Z, Xie S, Xu L, Du J, Li F. Her2-Functionalized Gold-Nanoshelled Magnetic Hybrid Nanoparticles: a Theranostic Agent for Dual-Modal Imaging and Photothermal Therapy of Breast Cancer. Nanoscale Res Lett. 2019;14(1):235.

25. Ray S, Li Z, Hsu CH, Hwang LP, Lin YC, Chou PT, Lin YY. Dendrimer- and copolymer-based nanoparticles for magnetic resonance cancer theranostics. Theranostics. 2018;8(22):6322-6349.

26. Mohammadzadeh P, Cohan RA, Ghoreishi SM, Bitarafan-Rajabi A, Ardestani MS. AS1411 Aptamer-Anionic Linear Globular Dendrimer G2-Iohexol Selective Nano-Theranostics. Sci Rep. 2017;7(1):11832.

27. Mirzaei M, Mohagheghi M, Shahbazi-Gahrouei D, Khatami A. Novel Nanosized Gd3+-ALGD-G2-C595: *In vivo* Dual Selective MUC-1 Positive Tumor Molecular MR Imaging and Therapeutic Agent. J Nanomed Nanotechol. 2012; 3:147.

28. Wängler C, Moldenhauer G, Eisenhut M, Haberkorn U, Mier W. Antibodydendrimer conjugates: the number, not the size of the dendrimers, determines the immunoreactivity. Bioconjug Chem. 2008;19 813-820.

29. Turyanskaya A, Rauwolf M, Pichler V, Simon R, Burghammer M, Fox OJL, Sawhney K, Hofstaetter JG, Roschger A, Roschger P, Wobrauschek P, Streli C. Detection and imaging of gadolinium accumulation in human bone tissue by micro- and submicro-XRF. Sci Rep. 2020;10(1):6301.

30. Jeong Y, Hwang HS, Na K. Theranostics and contrast agents for magnetic resonance imaging. Biomater Res. 2018; 22:20.

31. Assadi A, Najafabadi VS, Shandiz SA, Boroujeni AS, Ashrafi S, Vaziri AZ, Ghoreishi SM, Aghasadeghi MR, Ebrahimi SE, Pirali-Hamedani M, Ardestani MS. Novel chlorambucil-conjugated anionic linear-globular PEG-based second-generation dendrimer: *in vitro/in vivo* improved anticancer activity. Onco Targets Ther. 2016;9:5531-5543.

32. Abbasi E, Aval SF, Akbarzadeh A, Milani M, Nasrabadi HT, Joo SW, Hanifehpour Y, Nejati-Koshki K, Pashaei-Asl R. Dendrimers: synthesis, applications, and properties. Nanoscale Res Lett. 2014;9(1):247.

33. Nanjwade BK, Bechra HM, Derkar GK, Manvi FV, Nanjwade VK. Dendrimers: emerging polymers for drug-delivery systems. Eur J Pharm Sci. 2009;38(3):185-196.

306

Nanomed. J. 8(4): 298-306, Autumn 2021